HHS Public Access

Author manuscript

F S Sci. Author manuscript; available in PMC 2021 December 29.

Published in final edited form as:

F S Sci. 2021 November ; 2(4): 365–375. doi:10.1016/j.xfss.2021.09.001.

Blastocyst development after fertilization with in vitro spermatids derived from nonhuman primate embryonic stem cells

Sujittra Khampang, Ph.D.[a,b], **In Ki Cho, Ph.D.**[a,c,d], **Kanchana Punyawai, Ph.D.**[a], **Brittany Gill, B.S.**[c,d], **Jacqueline N. Langmo, B.S.**[c,d], **Shivangi Nath, Ph.D.**[g], **Katherine W. Greeson, B.S.**[c,d], **Krista M. Symosko, B.S.**[c,d], **Kristen L. Fowler, M.S.**[c,d], **Siran Tian, B.S.**[a], **John P. Statz, B.S.**[f,h], **Alyse N. Steves, Ph.D.**[a,d], **Rangsun Parnpai, Ph.D.**[b], **Michael A. White, Ph.D.**[g], **Jon D. Hennebold, Ph.D.**[f,h], **Kyle E. Orwig, Ph.D.**[e], **Calvin R. Simerly, Ph.D.**[e], **Gerald Schatten, Ph.D.**[e], **Charles A. Easley IV, Ph.D.**[a,c,d]

[a]Division of Neuropharmacology and Neurologic Diseases; Yerkes National Primate Research Center; Atlanta, Georgia;

[b]Embryo Technology and Stem Cell Research Center, School of Biotechnology, Suranaree University of Technology, Nakhon Ratchasima, Thailand;

[c]Department of Environmental Health Science, College of Public Health, University of Georgia; Athens, Georgia;

[d]Regenerative Bioscience Center; University of Georgia; Athens, Georgia;

[e]Magee-Womens Research Institute and Departments of Obstetrics, Gynecology, and Reproductive Sciences, Cell Biology and Bioengineering; University of Pittsburgh; Pittsburgh, Pennsylvania;

[f]Division of Reproductive and Developmental Sciences, Oregon National Primate Research Center, Beaverton, Oregon;

[g]Department of Genetics, University of Georgia, Athens, Georgia;

[h]Department of Obstetrics and Gynecology, Oregon Health and Science University, Portland, Oregon

Abstract

Objective: To demonstrate that functional spermatids can be derived in vitro from nonhuman primate pluripotent stem cells.

Reprint requests: Charles A. Easley IV, Ph.D., Department of Environmental Health Science, College of Public Health, 425 River Rd, Edgar Rhodes Animal and Dairy Sciences Rm 450, Athens, Georgia 30602 (cae25@uga.edu).

S.K. has nothing to disclose. I.K.C. has nothing to disclose. K.P. has nothing to disclose. B.G. has nothing to disclose. J.N.L. has nothing to disclose. S.N. has nothing to disclose. K.W.G. has nothing to disclose. K.M.S. has nothing to disclose. K.L.F. has nothing to disclose. S.T. has nothing to disclose. J.P.S. has nothing to disclose. A.N.S. has nothing to disclose. R.P. has nothing to disclose. M.A.W. has nothing to disclose. J.D.H. has nothing to disclose. K.E.O. has nothing to disclose. C.R.S. has nothing to disclose. G.S. has nothing to disclose. C.A.E. IV has nothing to disclose.

Design: Green fluorescent protein-labeled, rhesus macaque nonhuman primate embryonic stem cells (nhpESCs) were differentiated into advanced male germ cell lineages using a modified serum-free spermatogonial stem cell culture medium. In vitro-derived round spermatid-like cells (rSLCs) from differentiated nhpESCs were assessed for their ability to fertilize rhesus oocytes by intracytoplasmic sperm(atid) injection.

Setting: Multiple academic laboratory settings.

Patient(s): Not applicable.

Intervention(s): Intracytoplasmic sperm(atid) injection of in vitro-derived spermatids from nhpESCs into rhesus macaque oocytes.

Main Outcome Measure(s): Differentiation into spermatogenic cell lineages was measured through multiple assessments including ribonucleic acid sequencing and immunocytochemistry for various spermatogenic markers. In vitro spermatids were assessed for their ability to fertilize oocytes by intracytoplasmic sperm(atid) injection by assessing early fertilization events such as spermatid deoxyribonucleic acid decondensation and pronucleus formation/apposition. Preimplantation embryo development from the one-cell zygote stage to the blastocyst stage was also assessed.

Result(s): Nonhuman primate embryonic stem cells can be differentiated into advanced germ cell lineages, including haploid rSLCs. These rSLCs undergo deoxyribonucleic acid decondensation and pronucleus formation/apposition when microinjected into rhesus macaque mature oocytes, which, after artificial activation and coinjection of ten-eleven translocation 3 protein, undergo embryonic divisions with approximately 12% developing successfully into expanded blastocysts.

Conclusion(s): This work demonstrates that rSLCs, generated in vitro from primate pluripotent stem cells, mimic many of the capabilities of in vivo round spermatids and perform events essential for preimplantation development. To our knowledge, this work represents, for the first time, that functional spermatid-like cells can be derived in vitro from primate pluripotent stem cells.

Keywords

In vitro spermatogenesis; round spermatids; TET3; blastocysts

Male infertility is a global health issue, with some investigators raising concerns about a “sperm crisis” (1). Currently, approximately 15% of couples worldwide and approximately 12% of men in the United States are subfertile or infertile (2–4). The causes of male infertility include genetic defects, environmental toxicants, injuries, or medical treatments such as alkylating chemotherapies, which almost always result in sterility, especially in men (5–9). Regardless of the root cause, men who are unable to produce gametes useful in assisted reproductive technology are unable to father a child because no cures currently exist to treat their infertility.

Recent work by several laboratories, including our own, has demonstrated the ability to differentiate human pluripotent stem cells (hPSCs), including human embryonic stem cells

(hESCs), and human induced pluripotent stem cells (hiPSCs) into germ cell lineages (10–15). Some of these impactful studies have demonstrated the production of spermatogonia-like cells, primary and secondary spermatocyte-like cells, and haploid spermatid-like cells (10, 15). However, the “gold standard” (16) for producing functional gametes that could fertilize an oocyte could not be assessed in these studies because of ethical and legal concerns. Previous work in rodents has demonstrated the ability to produce live offspring from sperm cells generated by testicular grafts with primordial germ cells derived from mouse embryonic stem cells (11). Additionally, complete meiosis from differentiating mouse embryonic stem cells has been achieved (17). However, distinct biologic and kinetic differences between rodents and humans (18, 19) may prevent these exciting developments from being translated to humans. To test whether functional gametes can be derived in vitro from pluripotent stem cells, we used a system more relevant to humans: the nonhuman primate (NHP), rhesus macaque model. Unlike rodents, NHPs such as rhesus macaques share similar biologic mechanisms to human spermatogenesis, fertilization, early embryo, and fetal development (18, 19). Spermatogenesis in NHPs is also more kinetically similar to humans than rodents. Fertilization is also different in rodents vs. primates in that fertilization requires paternal centriole inheritance in both NHPs and humans but not in rodents (20–22). Taken together, the NHP models of spermatogenesis are more similar to humans than rodent models and, thus, represent an ideal and necessary model for exploring stem cell-based therapies for male infertility. In this study, to our knowledge, we demonstrate for the first time that male NHP pluripotent stem cells can differentiate into functional gametes that can fertilize NHP oocytes and develop to the blastocyst stage in vitro.

MATERIALS AND METHODS

NHP Embryonic Stem Cell Differentiation

A male rhesus macaque embryonic stem cell line (23), stably transduced with histone 2B (H2B)-green fluorescent protein (GFP), was differentiated into spermatogenic germ cell lineages, as previously described (10). For Supplemental Figure 2 (available online), the same nontransduced line was also differentiated, in addition to a rhesus induced pluripotent stem cell (nhpiPSC) line and a somatic cell nuclear transfer embryonic stem cell (nhpNT) line (validated [24]). Briefly, NHP pluripotent stem cell lines were cultured for 10 days on STO-feeder cells in mouse spermatogonial stem cell (SSC) medium containing the following: MEM α (Thermo Fisher), 0.2% bovine serum albumin (Sigma), 5 μg/mL of insulin (Sigma), 10 μg/mL of transferrin (Sigma), 60 μM of putrescine (Sigma), 2 mM of L-glutamine (Invitrogen), 50 μM of β-mercaptoethanol (Sigma), 1 ng/mL of human basic fibroblast growth factor (R&D Systems), 20 ng/mL of glial cell line-derived neurotrophic factor (R&D Systems), 30 nM of sodium selenite (Sigma), 2.36 μM of palmitic acid (Sigma), 0.21 μM of palmitoleic acid (Sigma), 0.88 μM of stearic acid (Sigma), 1.02 μM of oleic acid (Sigma), 2.71 μM of linoleic acid (Sigma), 0.43 μM of linolenic acid (Sigma), 10 mM of 4-(2-hydroxyethyl)-1-piperazineethane-sulfonic acid (HEPES [Sigma]), and 0.5× penicillin/streptomycin (Thermo Fisher). Cells were replenished with fresh medium every other day, and SSC medium was gassed with a blood gas mixture (5% CO_2, 5% O_2, 90% N_2 gas) before use. For comparison, in Supplemental Figure 2, nonhuman primate embryonic stem cell (nhpESC) H2B-GFP cells were differentiated with a bone morphogenetic protein

mixture, as described (12), without the addition of *DAZL*, *DAZ*, and *BOULE*. All NHP pluripotent stem cell lines were cultured as described (23) on mitomycin C inactivated mouse embryonic fibroblasts (Gibco) in Knockout DMEM (Gibco) medium containing 20% Knockout Serum Replacer (Gibco), 1 mM of L-glutamine (Gibco), 0.1 mM of nonessential amino acids (Gibco), 1% penicillin/streptomycin (Gibco), and 12 ng/mL of human recombinant basic fibroblast growth factor (PeproTech).

Extraction of Total Ribonucleic Acid

Total ribonucleic acid (RNA) was isolated from nhpESCs and differentiated cultures using the RNeasy Kit from Qiagen as per the manufacturer's instruction. Purified RNA samples were subjected to quality assessment using a NanoDrop (Thermo Fisher), in which the acceptable quality parameters were $OD_{260/230}$ greater than 1.9 and $OD_{260/280}$ greater than 2.0. Ribonucleic acid samples were divided into two aliquots for RNA sequencing (RNA-seq).

RNA-seq Data Analysis

Ribonucleic acid samples (nhpESC and three biologic replicates of SSC differentiations) were sent to Novogene for whole transcriptome RNA-seq (Novogene). Paired-end sequencing was conducted on Illumina NovaSeq 6000. The initial data analysis, including quality control and adapter sequence trimming, was performed at Novogene. The reference genome index of rhesus monkey was constructed using Spliced Transcripts Alignment to a Reference (v2.7.9a) with the latest release of rhesus monkey Ensembl genome assembly (build Mmul_10). Paired-end reads were aligned to the reference genome using Spliced Transcripts Alignment to a Reference RNA-seq alignment. Read counts were measured using featureCount (v2.0.1). Differential expression analyses of two cell types were performed on the Galaxy server (usegalaxy.org) using the edgeR method (Galaxy Version 3.24.1+galaxy1). The resulting *P* values were adjusted with the Benjamini–Hochberg method (false discovery rate) with the threshold set at .05. The normalization method used in this study was the trimmed mean of M-values. Differential expression analysis data and normalized read counts were used to generate graphs in RStudio (1.4.1717) running on R Package (R-4.1.0).

Round Spermatid Isolation, Oocyte Collection, and Intracytoplasmic Sperm(atid) Injection

Hyperstimulation of female rhesus monkeys exhibiting regular menstrual cycles was induced with exogenous gonadotropins. Beginning at menses, females were given recombinant human follicle-stimulating hormone (35 IU, intramuscular [i.m.]; Organon Inc.), administered twice daily for 6 days, followed by 1–3 days of recombinant human follicle-stimulating hormone + recombinant human luteinizing hormone (30 IU each, i.m.; Ares Serono), twice daily, and sub-cutaneous injections of a gonadotropin-releasing hormone antagonist (Acyline; Eunice Kennedy Shriver National Institute of Child Health and Development/National Institutes of Health; 75 mg/kg body weight), once daily. Ultrasonography was performed on day 7 of the stimulation to confirm adequate follicular response. When there were follicles 3–4 mm in diameter, an i.m. injection of 1,500 IU of recombinant human chorionic gonadotropin (Serono Laboratories, Inc., Randolph, MA) was administered for ovulation, and metaphase II oocytes were retrieved

at approximately 35 hours after recombinant human chorionic gonadotropin injection for intracytoplasmic sperm(atid) injection (ICSI) (25). This procedure was covered under Yerkes National Primate Research Center/Emory University Institutional Animal Care and Use Committee (approval no.: A3180–01) and the University of Georgia Animal Use Protocol (approval no.: A2019 02–009). Additionally, our animal studies were conducted in compliance with the Animal Research: Reporting of In Vivo Experiments guidelines (https://arriveguidelines.org/).

After 10-day differentiations, round spermatids were isolated by trypsinizing cultures and spotting cells into ICSI medium. Round spermatids were picked for ICSI using morphological characteristics outlined by Tanaka et al. (26, 27). In a vertical array, round spermatids were resuspended in 5-μL drops of SSC differentiation medium and placed onto a petri dish. A second 5-μL drop contained a mixture of 1 μL of ten-eleven translocation 3 (TET3) protein, 1 μL of TET3 plasmid deoxyribonucleic acid (DNA) (approximately 1 ng/μL), and 3 μL of sperm cytoplasmic factor (SCF) (28). The third 5-μL drop of Tyrode's lactate HEPES was placed at the bottom where oocytes were placed for ICSI. An ICSI micropipette (approximately 9 μm in inner diameter) was used to aspirate round spermatids, which were washed in a TET3–SCF mixture followed by cytoplasmic injection into metaphase II oocytes at a position 90° from the first polar body. After ICSI, fertilized oocytes were placed into Hamster Embryo Culture Medium (HECM-9) culture medium with 10 nM of trichostatin A (TSA; Sigma) for 10 hours, thoroughly washed, and placed in HECM-9 media for in vitro culture.

Haploid Cell Isolation, Cell Cycle Profiling, and Interphase Fluorescence In Situ Hybridization

To isolate haploid cells during fluorescence-activated cell sorting (FACS), differentiated H2B-GFP nhpESCs were trypsinized and stained with RedDot1 DNA stain (Biotium) as per the manufacturer's instructions in the SSC medium listed earlier. Haploid cells were then seeded on poly-d-lysine-coated coverslips and fixed with 4% paraformaldehyde before immunostaining.

For cell cycle profiling, the differentiated cultures were trypsinized and stained using the Cell Cycle Assay Kit for the MilliporeSigma Muse benchtop flow cytometer as per the manufacturer's instructions (Luminex).

To determine diploidy and haploidy on interphase cells, fluorescence in situ hybridization (FISH) analyses were conducted as previously described (29). Briefly, trypsinized differentiated nhpESC H2B-GFP cells or isolated haploid cells from the differentiations were pelleted and resuspended in 75-mM KCl and incubated for 10 minutes at 37 °C. Cells were then spun down at 200 × gram for 5 minutes at room temperature (RT) and fixed in Carnoy's fixative (3:1 methanol to glacial acetic acid) for 5 minutes on ice. This step was repeated two more times. In the final step, the cells were resuspended in approximately 200 μL of fixative and then dropped on the slides using a transfer pipette. The slides were allowed to dry at RT and then stored at RT for a short term until used for FISH. The slides were then permeabilized for 30 minutes in a permeabilization buffer containing 1× phosphate-buffered saline (PBS) solution, 1% Triton-X, and 10-mM

ethylenediaminetetraacetic acid at RT and then passed through an ethanol wash series of 70%, 85%, and 100%. The slides were then denatured at 75 °C for 5 minutes in denaturing solution (2× SSC, 70% formamide) and passed through the ethanol wash series again and left for drying at RT. The probe mix was prepared as per the manufacturer's instructions (GeneCopoeia, FITC probe for human chromosome 1) by combining 2 μL of probe solution and 8 μL of hybridization buffer. The probe mix was denatured at 75 °C for 5 minutes and kept on ice until the slides were completely dry. A diamond pencil was used to mark the position where probes were to be applied on the slides. Subsequently, 10 μL of probe mix was applied to the indicated position on slides and sealed with a square coverslip and rubber cement for overnight incubation at 37 °C. The following day, the slides were washed once in wash buffer 1 (2× SSC, 50% formamide, 0.1% TX-100) for 5 minutes and then in wash buffer 2 (2× SSC) for 5 minutes at 55 °C. After drying, the slides were sealed with VECTASHIELD with premixed 4′,6-diamidino-2-phenylindole.

Immunostaining

Nonhuman primate embryonic stem cells cultured in conditions defined earlier were immunostained as previously described (30). Briefly, samples were fixed in 4% paraformaldehyde (Sigma) for 15 minutes and then blocked with buffer containing 1× PBS (Thermo Fisher), 0.25% Triton-X (Sigma), 5% bovine serum albumin (Thermo Fisher), and 5% normal goat serum or donkey serum (Sigma) overnight at 4 °C. Primary antibody incubation occurred overnight at 4 °C in blocking buffer followed by three washes in 1× PBS with 0.25% Triton-X for 10 minutes each at RT. Secondary antibody (1:2000 dilution; Thermo Fisher) incubation was performed at RT for 2 hours, followed by three washes as described earlier. Samples were costained with Hoechst (Sigma). For FACS-obtained haploid cells, the isolated cells were seeded onto poly-d-lysine-coated coverslips for 10 minutes at 37 °C. Coverslips were then fixed in 4% paraformaldehyde and stained as described earlier. Additionally, rhesus testis cell suspensions were seeded onto poly-d-lysine-coated coverslips for 10 minutes at 37 °C (Supplemental Fig. 2). VASA (Supplemental Fig. 2), UTF1, SALL4, UCHL1, and PLZF antibodies were from R&D Systems (Supplemental Fig. 3 and 4). VASA (Supplemental Fig. 4), PIWIL1, and PIWIL2 antibodies were from Abcam. Acrosin (ACR), Protamine 1 (PRM1), and Transition Protein 1 were from Santa Cruz Biotechnology. Acetylated tubulin antibody was from Thermo Fisher. MAGEA4 and ID4 (Supplemental Fig. 4) were from Invitrogen/Thermo Fisher. All fluorescent secondary antibodies were from Thermo Fisher. All images shown are representative of at least five separate immunostaining experiments. For VASA+ counts, 5,000 cells were counted for each differentiation, and each differentiation was performed five times (n = 5). The percentages of total cell counts were calculated and averaged for the five trials.

Genomic Imprint Analyses for H19 and SNRPN

Genomic DNA from diploid nhpESCs and haploid cells obtained from FACS was isolated using the DNeasy Blood and Tissue kit from Qiagen following the manufacturer's instructions. Samples were prepared for imprint control region methylation analyses as previously described (30) with the EpiTect Methyl DNA Restriction Kit (Qiagen) as per the manufacturer's instructions. For quantitative polymerase chain reaction (qPCR)-based

analyses of imprint control region methylation for *H19* and *SNRPN* for each sample, the following EpiTect qPCR Methyl Promoter Primers were used: *H19*, catalog number 335002 EPHS102101–1A, and *SNRPN*, 335002 EPHS104389–1A. The percentage of methylation for *H19* and *SNRPN* imprint control regions was calculated for each sample as per the manufacturer's instructions (Qiagen).

In Vitro Transcription/Translation of TET3 and TET3 Gene Expression

Full-length human TET3 (FH-TET-pEF; Addgene#49446) plasmid DNA was used to generate TET3 protein supplements for ICSI. TET3 protein was generated using the Promega TnT (Transcription and Translation) kit as per the manufacturer's instructions. After the generation of TET3 protein, TET3 was immunopurified from the reticulocyte lysate using the Dynabeads Protein A Immunoprecipitation Kit (Thermo Fisher) as per the manufacturer's instructions using an immunoprecipitating-capable TET3 antibody (Abcam) with the following modification: immunoprecipitation was incubated overnight at 4 °C. After elution from Dynabeads, purified TET3 protein was diluted in a buffer (KCl 120 mM, HEPES 20 mM, EGTA 100 μM, sodium glycerophosphate 10 mM; pH 7.5) (28) compatible with ICSI.

TET3 RNA levels were measured in nhpESC; day 3, 5, 7, and 10 differentiation cultures; and mature wild-type sperm. Ribonucleic acid from all samples listed earlier was isolated using the RNeasy RNA Isolation Kit (Qiagen) as per the manufacturer's instructions. Complementary DNA (cDNA) was generated as described earlier using iScript Reverse Transcription Supermix for reverse transcription qPCR (Bio-Rad) as per the manufacturer's instructions. Three distinct biologic replicates were used for analyses with average normalized fold change ($2^{-\delta\delta CT}$) shown. Polymerase chain reaction primer sequences for TET3 were as follows: forward, 5′-CCCAAAGAGGAAGAAGTG-3′, and reverse, 5′-GCAGTCAATCGCTATTTC-3′.

Embryo Development Assessments

Fertilized embryos were cultured in HECM-9 media (25) and were monitored daily until days 7–8 when blastocysts were formed. To minimize fluorescent light exposure that may affect embryo development, selected embryos were used for fluorescent imaging. The embryo development rates were calculated on the basis of fertilized embryos that had achieved the first division, 4–8-cell, 16-cell, morula, compacted morula, blastocyst, and expanded blastocyst stages.

Embryo Fragmentation, Whole Genome Amplification, and Genotyping

Embryos derived from rhesus macaque oocytes fertilized by in vitro rSLfro Cs m nhpESC H2B-GFP cells were fragmented and genotyped as previously described (31). Briefly, zona pellucidas were removed from each embryo by exposure to acidified Tyrode's solution (EMD Millipore) and washed with Ca^{2+}- and Mg^{2+}-free PBS. Embryos were disaggregated with Quinn's advantage Ca^{2+}- and Mg^{2+}-free medium with HEPES plus 10% human albumin (CooperSurgical) and 0.05% trypsin–ethylenediaminetetraacetic acid (Thermo Fisher) as necessary. Each blastomere was washed with Ca^{2+}- and Mg^{2+}-free PBS and collected individually for transfer to a sterile UltraFlux PCR tube (VWR).

All of the aforementioned were performed under a stereomicroscope equipped with a digital camera (Leica Microsystems) to document every sample collection. Samples were put into tubes, flash-frozen on dry ice, and stored at −80 °C. Only embryos for which the disassembly process occurred effectively with no apparent loss of material were carried forward for library preparation and sequencing. Deoxyribonucleic acid from individual blastomeres was isolated, and whole genome amplification was performed using Qiagen's REPLI-g Single Cell Kit as per the manufacturer's instruction. Genotyping PCR was performed for GFP using validated primers for GFP from Integrated DNA Technologies: *GFP* forward, 5′-AAGCTGACCCTGAAGTTCATCTGC-3′, and reverse, 5′-CTTG TAGTTGCCGTCGTCCTTGAA-3′. Two additional primer sets were used to confirm whole genome amplification: *MYO7A* forward, 5′-GAGTGGTGTCCCTGTGAGGA-3′, and reverse, 5′-GTCTGAGGAGCTTCTAGCCTG-3′, and *CNGB3* forward, 5′-ACTTGCACCAAAACCTCTAGT-3′, and reverse, 5′-GCTTCAAAAACACTGGCTCTCA-3′.

Statistics

Two-tailed, unequal variance *t* tests were performed to establish significance for various experiments within this study. Significance was determined as $P<.05$. Graphical analyses shown are indicative of average values ± standard deviation. For all experiments, greater than three trials were performed, and data are representative of all trials. For *TET3* gene expression data analysis, normalized gene expression was calculated by subtracting the relative expression of *TET3* from *GAPDH* of each sample to H2B ESC, and fold expression was calculated using the $\delta\delta$Ct method. A one-way analysis of variance with the Tukey post hoc analysis was calculated for pair-wise comparisons to determine the statistical significance. All samples were calculated with three biologic replicates, and $P<.05$ was considered statistically significant. Computations were performed using Prism 9.

RESULTS

nhpESCs Can Be Differentiated into Spermatogenic Cells

Previously, we demonstrated the ability to differentiate hESCs and hiPSCs into advanced spermatogenic cells, including spermatogonia-like cells, primary spermatocyte-like cells, secondary spermatocyte-like cells, and haploid round spermatid-like cells (rSLCs) by culturing hPSCs in mouse SSC growth conditions (10). This work has since been independently replicated (15), highlighting the reproducibility of our methodology. To first determine whether nhpESCs differentiate into spermatogenic cells similar to hESCs and hiPSCs, we differentiated nhpESCs in mouse SSC culture conditions as previously described (10, 15, 30, 32–36). We chose nhpESC H2B-GFP line for downstream analyses, but all lines tested (Supplemental Fig. 2) differentiated into spermatogonia-like cells, primary and secondary spermatocyte-like cells, and haploid spermatid-like cells similarly to hESCs and hiPSCs (10) (Figs. 1 and 2, Supplemental Figs. 1, 2–4). Using the nhpESC H2B-GFP line, we performed RNA-seq analyses on undifferentiated cells and differentiated cells from three differentiations. Both principal component analysis and Poisson distance plot analysis showed that nhpESCs are distinctly different from our three differentiations, whereas the differentiations cluster together (Fig. 1A and B). Similarly, when all permutations of

sample pairs were compared, all three of our biologic replicates showed a large number of differentially expressed genes compared with nhpESCs (Supplemental Figs. 1A to C). Comparisons among differentiations from different passage numbers showed some variations in spermatogenic gene expression (Supplemental Fig. 1D and 2B, Fig. 1A); however, different dishes from the same passage number showed no statistically significant difference in expression levels (Supplemental Fig. 1F). Differential gene expression analysis (DeSeq2) showed 1,875 upregulated and 1,431 downregulated genes between nhpESCs and our differentiations (Fig. 1C). Of the 1,875 genes upregulated in our in vitro differentiations, we observed up-regulation of genes involved in spermatogenesis, including *PAX6*, *GFRA1*, *DMRT1*, and *ZBTB16* (Fig. 1D). In contrast, the expressions of genes critical for maintaining pluripotency, *POU5F1*, *SPP1*, and *MYC*, were significantly downregulated (Fig. 1D). We next generated a heatmap of genes in the spermatogenesis gene set (GO:0048515) and observed an enrichment of gene expression in our differentiated cells (Fig. 1E). To further examine the ability to differentiate nhpESCs into spermatogenic cells, we evaluated several spermatogenic markers by immunocytochemistry. Differentiation of nhpESCs in mouse SSC culture conditions for 10 days showed significant increases in VASA protein expression compared with cells differentiated for 14 days in a previously published protocol using a bone morphogenetic protein cocktail (Supplemental Fig. 2A). The 10-day differentiation of nhpESC H2B-GFP cells resulted in cells expressing the undifferentiated spermatogonia marker PLZF, the differentiating spermatogonia marker UTF1, the primary spermatocyte marker PIWIL2, and the secondary spermatocyte marker PIWIL1, as shown by immunocytochemistry (Supplemental Fig. 3). Differentiating nhpESC H2B-GFP cells also expressed SALL4, MAGEA4, ID4, UCHL1, and VASA as shown by immunocytochemistry (Supplemental Fig. 4). Secondary antibody-only immunostaining demonstrated the specificity of our antibody staining (Supplemental Fig. 4).

Differentiating nhpESCs Yield Haploid rSLCs

In our previous work, we demonstrated that rSLCs could be produced from hESCs and hiPSCs (10, 30, 35, 36). To determine if nhpESCs could be differentiated into rSLCs similar to hPSCs, we differentiated nhpESC H2B-GFP cells in SSC conditions for 10 days. In examining our entire differentiation cultures, which included spermatogonia-like cells, primary spermatocyte-like cells, secondary spermatocyte-like cells in addition to rSLCs, we observed a haploid cell population averaging approximately 5.3% across multiple differentiations (Fig. 2A). On sorting this haploid peak (indicated by the asterisk), we confirmed haploidy by FISH for human chromosome 1 (which has high homology to rhesus chromosome 1) in FACS-isolated rSLCs compared with diploid spermatogenic cells (Fig. 2B). We further analyzed in vitro-derived and FACS-isolated rSLCs for the expression of spermatid-related markers. All rSLCs demonstrated the expression of ACR, PRM1, and Transition Protein 1 (Fig. 2C). Round spermatid-like cells also showed morphological similarities to endogenous NHP round spermatids, including cytoplasmic and nuclear localization of PRM1 (Fig. 2D and Supplemental Fig. 5E and F), which colocalizes to the cytoplasm and nucleus during the round spermatid stage in vivo (37). Additionally, rSLCs showed proper imprint establishment on two confirmed parent-of-origin imprints in NHPs (38, 39) (Supplemental Fig. 5A to D). In addition to the nhpESC H2B-GFP line, other NHP lines showed a similar ability to produce haploid spermatids that express

ACR (Supplemental Fig. 2D). Taken together, these results demonstrate that we are able to differentiate NHP pluripotent stem cell lines into advanced spermatogenic lineages, including rSLCs.

rSLCs Derived from nhpESCs Are Functional but Require Oocyte Activation

Like in our previous study using hESCs and hiPSCs (10), our nhpESC-derived spermatogenic cells, including rSLCs, exhibited many of the hallmarks of the "gold standards" (16) of in vitro-derived gametes. The highest stringency test for in vitro-derived gametes is the ability to fertilize oocytes and produce embryos. However, we were unable to assess the functionality of rSLCs derived from hESCs and hiPSCs because of ethical and legal considerations. To explore whether NHP in vitro-derived rSLCs have functional gamete ability, we fertilized rhesus oocytes by ICSI (as an example, Supplemental Fig. 5G and H). Similar to clinical assisted reproductive technology applications using endogenous round spermatids, our in vitro-derived rSLCs could not activate oocytes for in vitro development. However, these rSLCs underwent DNA decondensation and pronucleus formation, generally arresting at the four- to eight-cell developmental stage (Fig. 3A to F and Supplemental Fig. 6A and B). On oocyte activation using a crude sperm extract (40), ICSI of NHP rSLCs derived from nhpESC H2B-GFP induced further development, DNA decondensation, male and female pronucleus formation, and cleavage (Fig. 3A to F). While most embryos arrested at the 8–16-cell stage, the stage where NHPs undergo maternal to zygotic transcription control, some progressed to the blastocyst stage (Supplemental Fig. 6A and B). The H2B-GFP expression in the nuclei of cells throughout the developing embryo demonstrates that the male genome from the nhpESC-derived rSLCs contributed to the developing embryo (Fig. 3).

Because most of the embryos arrested at the 8–16-cell stage, when the embryonic genome engages, we hypothesized that DNA demethylation was not readily occurring on the male genome. As such, we examined whether in vitro-derived rSLCs lacked TET3, an enzyme responsible for DNA demethylation on the male pronucleus, which is a critical step in early fertilization (41, 42). Like endogenous round spermatids and unlike mature sperm, our in vitro-derived rSLCs show reduced *TET3* expression (Fig. 4A). The addition of purified TET3 protein and TSA at the time of rSLC injection significantly improved the fertilization rates, improved embryo morphology, and elevated the blastocyst rates compared with *TET3* cDNA + TSA, *TET3* cDNA + mRNA + TSA, or oocyte activation alone (Fig. 4B to H and Supplemental Fig. 6A to E). Additionally, we confirmed that the H2B-GFP transgene contributed to fertilization and embryo development through the visualization of GFP throughout the embryo (Fig. 3G to I) and by genotyping fractionated embryos for the GFP transgene (Supplemental Fig. 6F). Our results indicated that not only was GFP fluorescence observed throughout the embryo but the transgene was present in every blastomere where DNA was amplified (Fig. 3G to I and Supplemental Fig. 6F). Taken together, these results show for the first time that functional rSLCs can be generated in vitro from primate pluripotent stem cells. However, these rSLCs require oocyte activation and TET3 protein supplementation to produce high-quality embryos.

DISCUSSION

Recent advancements in patient-specific induced pluripotent stem cell technology have led to suggestions of generating male germ cells by in vitro gametogenesis. However, the successful production of functional male gametes in vitro has only previously been accomplished in mice, with no reports in higher mammals, including primates. Here, for the first time, we present evidence showing that functional haploid spermatids can be differentiated from NHP pluripotent stem cells completely in vitro. Specifically, we demonstrate that NHP pluripotent stem cells can be differentiated into spermatogenic lineages, including spermatid-like cells that can fertilize an NHP oocyte and develop to the blastocyst stage.

While the results shown here represent a significant step in generating male germ cells in vitro, several concerns still exist. Among the concerns remaining to be resolved comprehensively, it is important to note that the derived spermatid-like cells, like in vivo primate round spermatids, are immature and not capable of activating mature oocytes on their own. To overcome this hurdle for fertilization, the addition of activation factors coupled with purified TET3 protein increases the efficiency of generating healthy embryos. One caveat is the potential production of parthenogenetic embryos as a result of our oocyte activation procedure. The derivation of rhesus parthenogenetic embryos to blastocysts has been accomplished but generally requires specific exogenous factors in addition to oocyte activation, such as inhibitors that block protein synthesis or protein phosphorylation. Even under these optimized conditions, several in vitro-derived rhesus parthenogenetic blastocysts are of low quality, with small inner cell masses, fail to fully expand the blastocoel, and show extruded blastomeres in the blastocoelic cavity, owing to high levels of apoptosis (43–45). We did not observe such phenotypes in blastocysts produced by our activation protocol combined with the injection of in vitro-derived spermatids and/or purified TET3. Evidence that the resulting blastocysts are not of parthenogenetic origin includes the integration of the male genome as determined by PCR analyses and the presence of GFP fluorescence in the nuclei of cells within the embryo. Instead, the addition of TET3, which is typically expressed in mature sperm, helps overcome the developmental arrests when injecting in vitro-derived rSLCs into rhesus oocytes. Another concern is how faithfully our model replicates in vivo meiosis. We and others have demonstrated the expression of meiotic markers such as SYCP3 (10, 15) and confirmed haploidy by FISH. While preliminary, these results highlight that some of the meiotic machinery is engaged to produce haploid rSLCs in vitro. As research continues to advance spermatogenesis/spermiogenesis in vitro to derive more mature spermatozoa, our protocol provides an investigative opportunity for understanding the mechanisms of this crucial biologic process. Additionally, this work may even help bridge the fields of reproductive and developmental biology by providing insights into why spermatogenesis arrests in certain male patients with infertility.

CONCLUSION

Here we demonstrate the differentiation of NHP pluripotent stem cells into advanced spermatogenic cells, including postmeiotic rSLCs. Like in vivo round spermatids, in vitro-derived rSLCs cannot activate oocytes during ICSI but instead require exogenous oocyte

activation. The addition of TET3 coupled with oocyte activation further improved the embryo development rates when ICSI was performed with in vitro-derived rSLCs. These combined results demonstrate for the first time the ability to produce functional gametes in vitro from NHP pluripotent stem cells.

Supplementary Material

Refer to Web version on PubMed Central for supplementary material.

Acknowledgments:

The authors kindly thank Dr. Anthony Chan, Center for Scientific Review National Institutes of Health, for his previous support and guidance while he was a faculty member at the Yerkes National Primate Research Center.

Supported by NIH/OD grant R21OD020182 (to C.A.E.); NIH/OD grant P51OD011092 (to J.D.H.); NIH/OD grant R01OD028223-01 (to C.A.E. and K.E.O.); and SUT-PhD/02/2556 scholarship (to S.K. and R.P.).

REFERENCES

1. Levine H, Jorgensen N, Martino-Andrade A, Mendiola J, Weksler-Derri D, Mindlis I, et al. Temporal trends in sperm count: a systematic review and meta-regression analysis. Hum Reprod Update 2017;23:646–59. [PubMed: 28981654]
2. Chandra A, Copen CE, Stephen EH. Infertility and impaired fecundity in the United States, 1982–2010: data from the National Survey of Family Growth. Natl Health Stat Report 2013:1–18, 1 p following 9.
3. Gassei K, Orwig KE. Experimental methods to preserve male fertility and treat male factor infertility. Fertil Steril 2016;105:256–66. [PubMed: 26746133]
4. Louis JF, Thoma ME, Sorensen DN, McLain AC, King RB, Sundaram R, et al. The prevalence of couple infertility in the United States from a male perspective: evidence from a nationally representative sample. Andrology 2013;1: 741–8. [PubMed: 23843214]
5. Bahadur G Fertility issues for cancer patients. Mol Cell Endocrinol 2000; 169:117–22. [PubMed: 11155943]
6. Deutsch MA, Kaczmarek I, Huber S, Schmauss D, Beiras-Fernandez A, Schmoeckel M, et al. Sirolimus-associated infertility: case report and literature review of possible mechanisms. Am J Transplant 2007;7:2414–21. [PubMed: 17845575]
7. Schlegel PN. Evaluation of male infertility. Minerva Ginecol 2009;61: 261–83. [PubMed: 19745794]
8. Skrzypek J, Krause W. Azoospermia in a renal transplant recipient during sirolimus (rapamycin) treatment. Andrologia 2007;39:198–9. [PubMed: 17714220]
9. Wallace WH. Oncofertility and preservation of reproductive capacity in children and young adults. Cancer 2011;117:2301–10. [PubMed: 21523750]
10. Easley CA 4th, Phillips BT, McGuire MM, Barringer JM, Valli H, Hermann BP, et al. Direct differentiation of human pluripotent stem cells into haploid spermatogenic cells. Cell Rep 2012;2:440–6. [PubMed: 22921399]
11. Hayashi K, Ohta H, Kurimoto K, Aramaki S, Saitou M. Reconstitution of the mouse germ cell specification pathway in culture by pluripotent stem cells. Cell 2011;146:519–32. [PubMed: 21820164]
12. Kee K, Angeles VT, Flores M, Nguyen HN, Reijo Pera RA. Human DAZL, DAZ and BOULE genes modulate primordial germ-cell and haploid gamete formation. Nature 2009;462:222–5. [PubMed: 19865085]
13. Panula S, Medrano JV, Kee K, Bergstrom R, Nguyen HN, Byers B, et al. Human germ cell differentiation from fetal- and adult-derived induced pluripotent stem cells. Hum Mol Genet 2011;20:752–62. [PubMed: 21131292]

14. Park TS, Galic Z, Conway AE, Lindgren A, van Handel BJ, Magnusson M, et al. Derivation of primordial germ cells from human embryonic and induced pluripotent stem cells is significantly improved by coculture with human fetal gonadal cells. Stem Cells 2009;27:783–95. [PubMed: 19350678]
15. Zhao Y, Ye S, Liang D, Wang P, Fu J, Ma Q, et al. In vitro modeling of human germ cell development using pluripotent stem cells. Stem Cell Reports 2018; 10:509–23. [PubMed: 29398481]
16. Handel MA, Eppig JJ, Schimenti JC. Applying "gold standards" to in-vitro-derived germ cells. Cell 2014;157:1257–61. [PubMed: 24906145]
17. Zhou Q, Wang M, Yuan Y, Wang X, Fu R, Wan H, et al. Complete meiosis from embryonic stem cell-derived germ cells in vitro. Cell Stem Cell 2016; 18:330–40. [PubMed: 26923202]
18. Ehmcke J, Wistuba J, Schlatt S. Spermatogonial stem cells: questions, models and perspectives. Hum Reprod Update 2006;12:275–82. [PubMed: 16446319]
19. Fayomi AP, Orwig KE. Spermatogonial stem cells and spermatogenesis in mice, monkeys and men. Stem Cell Res 2018;29:207–14. [PubMed: 29730571]
20. Navara CS, Simerly C, Zoran S, Schatten G. The sperm centrosome during fertilization in mammals: implications for fertility and reproduction. Reprod Fertil Dev 1995;7:747–54. [PubMed: 8711211]
21. Schatten G, Simerly C. LEGOs® and legacies of centrioles and centrosomes. EMBO Rep 2015;16:1052–4. [PubMed: 26249334]
22. Simerly C, Wu GJ, Zoran S, Ord T, Rawlins R, Jones J, et al. The paternal inheritance of the centrosome, the cell's microtubule-organizing center, in humans, and the implications for infertility. Nat Med 1995;1:47–52. [PubMed: 7584952]
23. Navara CS, Mich-Basso JD, Redinger CJ, Ben-Yehudah A, Jacoby E, Kovkarova-Naumovski E, et al. Pedigreed primate embryonic stem cells express homogeneous familial gene profiles. Stem Cells 2007;25:2695–704. [PubMed: 17641389]
24. Byrne JA, Pedersen DA, Clepper LL, Nelson M, Sanger WG, Gokhale S, et al. Producing primate embryonic stem cells by somatic cell nuclear transfer. Nature 2007;450:497–502. [PubMed: 18004281]
25. Arthur Chang TC, Chan AW. Assisted reproductive technology in nonhuman primates. Methods Mol Biol 2011;770:337–63. [PubMed: 21805271]
26. Tanaka A, Nagayoshi M, Takemoto Y, Tanaka I, Kusunoki H, Watanabe S, et al. Fourteen babies born after round spermatid injection into human oocytes. Proc Natl Acad Sci U S A 2015;112:14629–34. [PubMed: 26575628]
27. Tanaka A, Suzuki K, Nagayoshi M, Tanaka A, Takemoto Y, Watanabe S, et al. Ninety babies born after round spermatid injection into oocytes: survey of their development from fertilization to 2 years of age. Fertil Steril 2018; 110:443–51. [PubMed: 30098696]
28. Simerly CR, Navara CS. Nuclear transfer in the rhesus monkey: opportunities and challenges. Cloning Stem Cells 2003;5:319–31. [PubMed: 14733750]
29. Howe B, Umrigar A, Tsien F. Chromosome preparation from cultured cells. J Vis Exp 2014:e50203. [PubMed: 24513647]
30. Greeson KW, Fowler KL, Estave PM, Kate Thompson S, Wagner C, Clayton Edenfield R, et al. Detrimental effects of flame retardant, PBB153, exposure on sperm and future generations. Sci Rep 2020;10:8567. [PubMed: 32444626]
31. Daughtry BL, Rosenkrantz JL, Lazar NH, Fei SS, Redmayne N, Torkenczy KA, et al. Single-cell sequencing of primate preimplantation embryos reveals chromosome elimination via cellular fragmentation and blastomere exclusion. Genome Res 2019;29:367–82. [PubMed: 30683754]
32. Easley CAt, Bradner JM, Moser A, Rickman CA, McEachin ZT, Merritt MM, et al. Assessing reproductive toxicity of two environmental toxicants with a novel in vitro human spermatogenic model. Stem Cell Res 2015;14: 347–55. [PubMed: 25863443]
33. Steves AN, Bradner JM, Fowler KL, Clarkson-Townsend D, Gill BJ, Turry AC, et al. Ubiquitous flame-retardant toxicants impair spermatogenesis in a human stem cell model. iScience 2018;3:161–76. [PubMed: 29901031]

34. Steves AN, Turry A, Gill B, Clarkson-Townsend D, Bradner JM, Bachli I, et al. Per- and polyfluoroalkyl substances impact human spermatogenesis in a stem-cell-derived model. Syst Biol Reprod Med 2018;64:225–39. [PubMed: 29911897]

35. Correll-Tash S, Lilley B, Salmons Iv H, Mlynarski E, Franconi CP, McNamara M, et al. Double strand breaks (DSBs) as indicators of genomic instability in PATRR-mediated translocations. Hum Mol Genet 2021;29:3872–81. [PubMed: 33258468]

36. Khampang S, Parnpai R, Mahikul W, Easley CA 4th, Cho IK, Chan AWS. CAG repeat instability in embryonic stem cells and derivative spermatogenic cells of transgenic Huntington's disease monkey. J Assist Reprod Genet 2021;38:1215–29. [PubMed: 33611676]

37. Carrell DT, Emery BR, Hammoud S. Altered protamine expression and diminished spermatogenesis: what is the link? Hum Reprod Update 2007;13: 313–27. [PubMed: 17208950]

38. Fujimoto A, Mitalipov SM, Clepper LL, Wolf DP. Development of a monkey model for the study of primate genomic imprinting. Mol Hum Reprod 2005; 11:413–22. [PubMed: 15908455]

39. Fujimoto A, Mitalipov SM, Kuo HC, Wolf DP. Aberrant genomic imprinting in rhesus monkey embryonic stem cells. Stem Cells 2006;24:595–603. [PubMed: 16269527]

40. Meng L, Wolf DP. Sperm-induced oocyte activation in the rhesus monkey: nuclear and cytoplasmic changes following intracytoplasmic sperm injection. Hum Reprod 1997;12:1062–8. [PubMed: 9194667]

41. Guo F, Li X, Liang D, Li T, Zhu P, Guo H, et al. Active and passive demethylation of male and female pronuclear DNA in the mammalian zygote. Cell Stem Cell 2014;15:447–59. [PubMed: 25220291]

42. Ni K, Dansranjavin T, Rogenhofer N, Oeztuerk N, Deuker J, Bergmann M, et al. TET enzymes are successively expressed during human spermatogenesis and their expression level is pivotal for male fertility. Hum Reprod 2016; 31:1411–24. [PubMed: 27141042]

43. Daughtry B, Mitalipov S. Concise review: parthenote stem cells for regenerative medicine: genetic, epigenetic, and developmental features. Stem Cells Transl Med 2014;3:290–8. [PubMed: 24443005]

44. Dighe V, Clepper L, Pedersen D, Byrne J, Ferguson B, Gokhale S, et al. Heterozygous embryonic stem cell lines derived from nonhuman primate parthenotes. Stem Cells 2008;26:756–66. [PubMed: 18192229]

45. Mitalipov SM, Nusser KD, Wolf DP. Parthenogenetic activation of rhesus monkey oocytes and reconstructed embryos. Biol Reprod 2001; 65:253–9. [PubMed: 11420247]

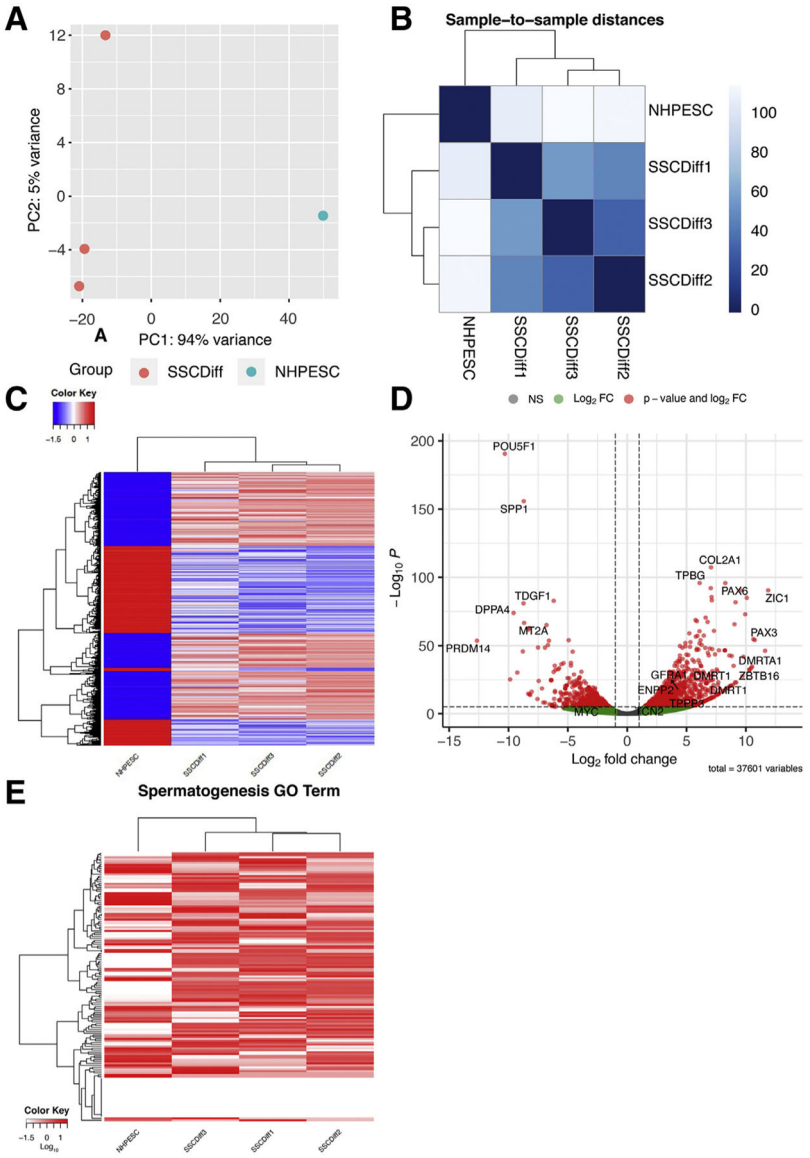

FIGURE 1.

Ribonucleic acid sequencing analysis of in vitro-directed differentiation of nonhuman primate embryonic stem cells (nhpESCs) into spermatogenic cells. (**A**) Principal component analysis plot of three biologic replicates after differentiation (*red*) and their base nhpESC histone 2B-green fluorescent protein cells (*blue*). (**B**) Poisson distance plot showing sample dissimilarities based on the transcriptome profiles. (**C**) Heatmap of hierarchical clustering of significantly differentially expressed genes of nhpESC and three biologic replicates of differentiated spermatogenic cells (SSCDiffs) showing 1,875 upregulated and 1,431 downregulated genes. (**D**) Volcano plot presenting differentially expressed genes that show either ± twofold change (*green*) or *P* values less than 10^{-6} (*red*). The most significantly differentially expressed genes are denoted on the plot: pluripotency genes (*POU5F1*, *SPP1*, and *MYC*) among downregulated genes and spermatogenesis genes (*PAX6*, *GFRA1*, *DMRT1*, and *ZBTB16*) among upregulated genes. (**E**) Heatmap of genes in

a spermatogenesis gene set (GO:0048515) from Gene Set Enrichment Analysis of nhpESC and all three biologic replicates of differentiated spermatogenic cells. Each heatmap (**C**, **E**) represents Log_{10}+1 normalized gene expression by edgeR normalized by each row.

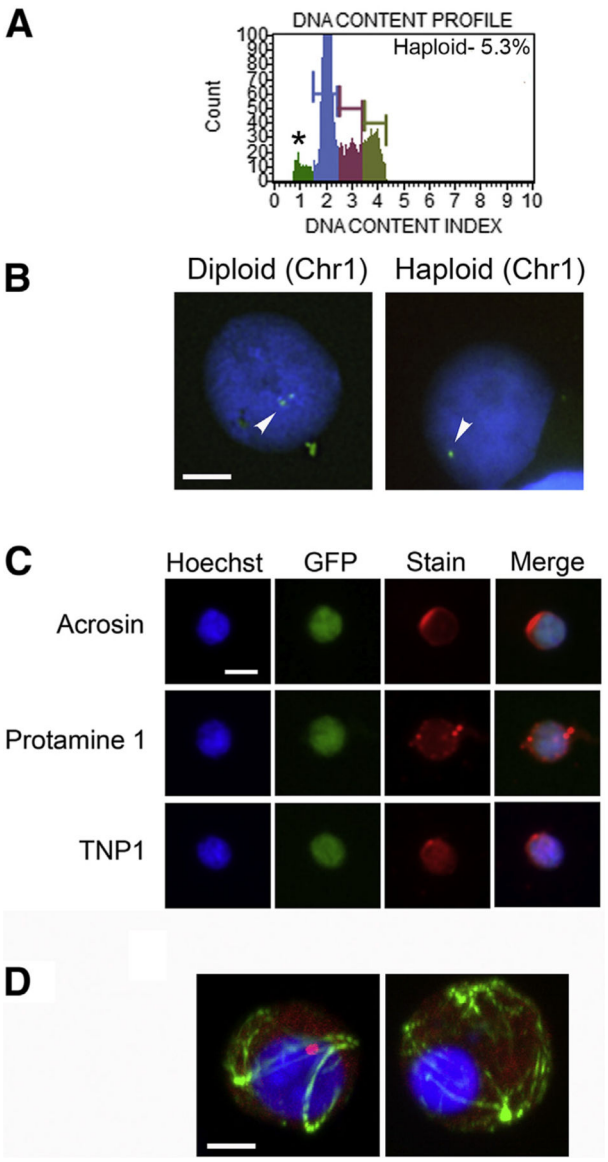

FIGURE 2.

Nonhuman primate embryonic stem cell (nhpESC) histone 2B-green fluorescent protein (H2B-GFP) cells differentiated in spermatogonial stem cell (SSC) conditions yield haploid, round spermatid-like cells. (**A**) Representative cell cycle flow cytometry profile data from one of five separate differentiations (n = 5) (*left image*) of nhpESC H2B-GFP cells differentiated in SSC conditions for 10 days. The dark green peak on the left-hand side of the graph represents the 1N peak (*asterisk*). (**B**) Fluorescence in situ hybridization (FISH) confirms haploidy. Representative FISH images from five different (n = 5) nhpESC H2B-GFP cells differentiated for 10 days in SSC conditions. The FISH Probe for chromosome 1 (*green*) shows a diploid cell (*left image*) with two chromosome 1s (*arrow* indicating two *green dots*), and sorted haploid cells (*right image*) show one chromosome 1 *(arrow* indicating one *green dot*). Bar = 5 μm. (**C**) Following our 10-day differentiation, haploid cells were sorted by fluorescence-activated cell sorting and immunostained with antibodies

against postmeiotic spermatid markers (*red*, *third column*) acrosin (*top row*), Protamine 1 (PRM1; *middle row*), and Transition Protein 1 (TNP1; *bottom row*). H2B-GFP (*green*, *second column*); Hoechst stain (*blue*, *first column*) for deoxyribonucleic acid. Merge of fluorescence images (*fourth column*). Bar = 10 μm. Data shown are representative of five separate differentiations (n = 5). (**D**) Representative images of round spermatids from a rhesus testis cell biopsy (*left*) and an in vitro-derived round spermatid-like cell (*right*) stained with 4′,6-diamidino-2-phenylindole (*blue*), Protamine 1 (*red*), and acetylated tubulin (*green*). Bar = 5 μm.

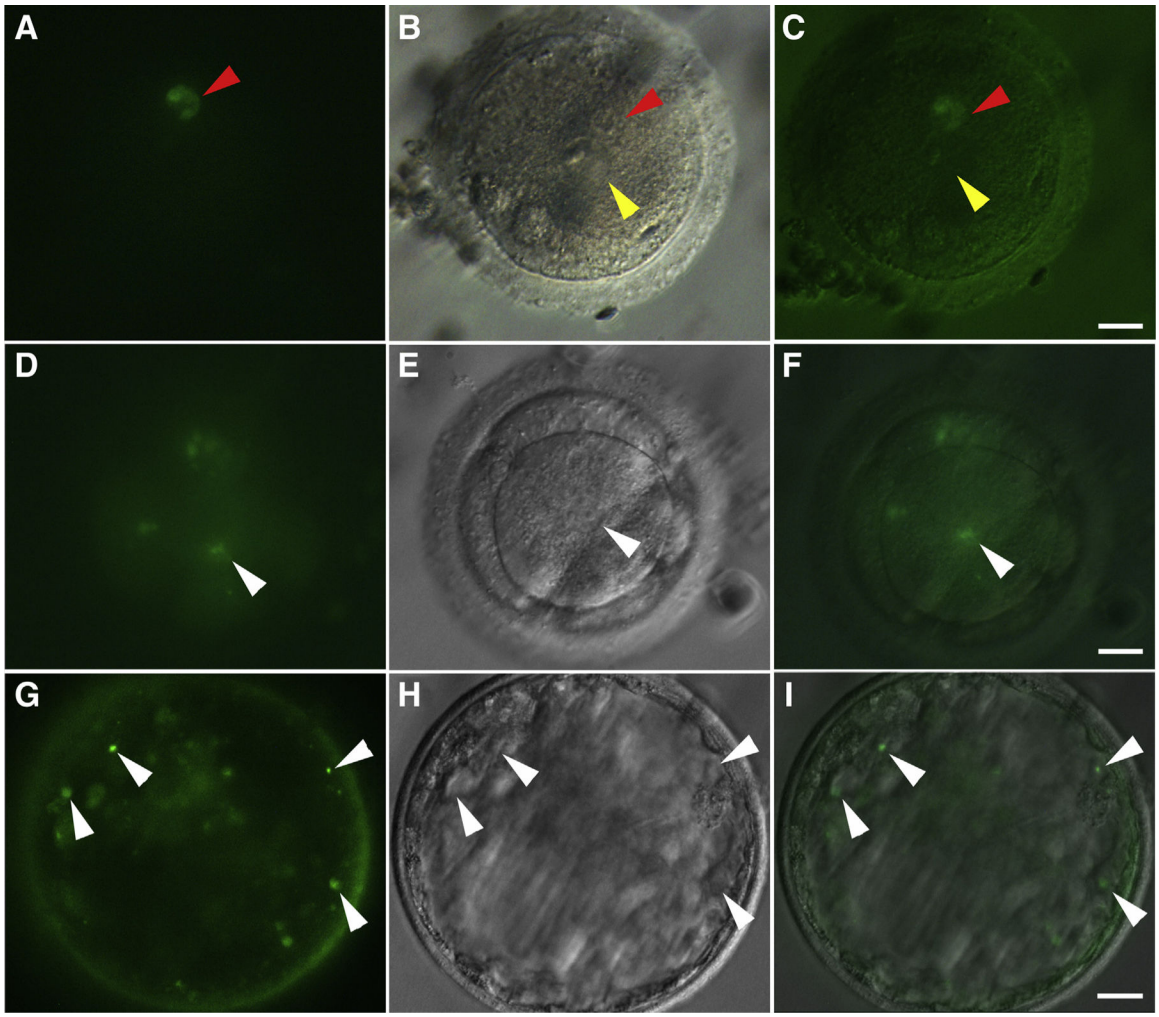

FIGURE 3.

Successful fertilization of rhesus oocytes by in vitro-derived round spermatid-like cells from nonhuman primate embryonic stem cell histone 2B-green fluorescent protein (GFP) cells differentiated in spermatogonial stem cell conditions for 10 days. (**A**–**C**) One-cell embryo with male pronucleus expressing GFP; (**D**–**F**) four-cell embryo with GFP expressing nuclei; (**G**–**I**) blastocyst expressing GFP from in vitro-derived spermatids. Red arrowhead, paternal pronucleus expressing GFP. Yellow arrowhead, maternal pronucleus with no GFP. White arrowheads, blastomeres and their nuclei expressing GFP. Bar = 15 um.

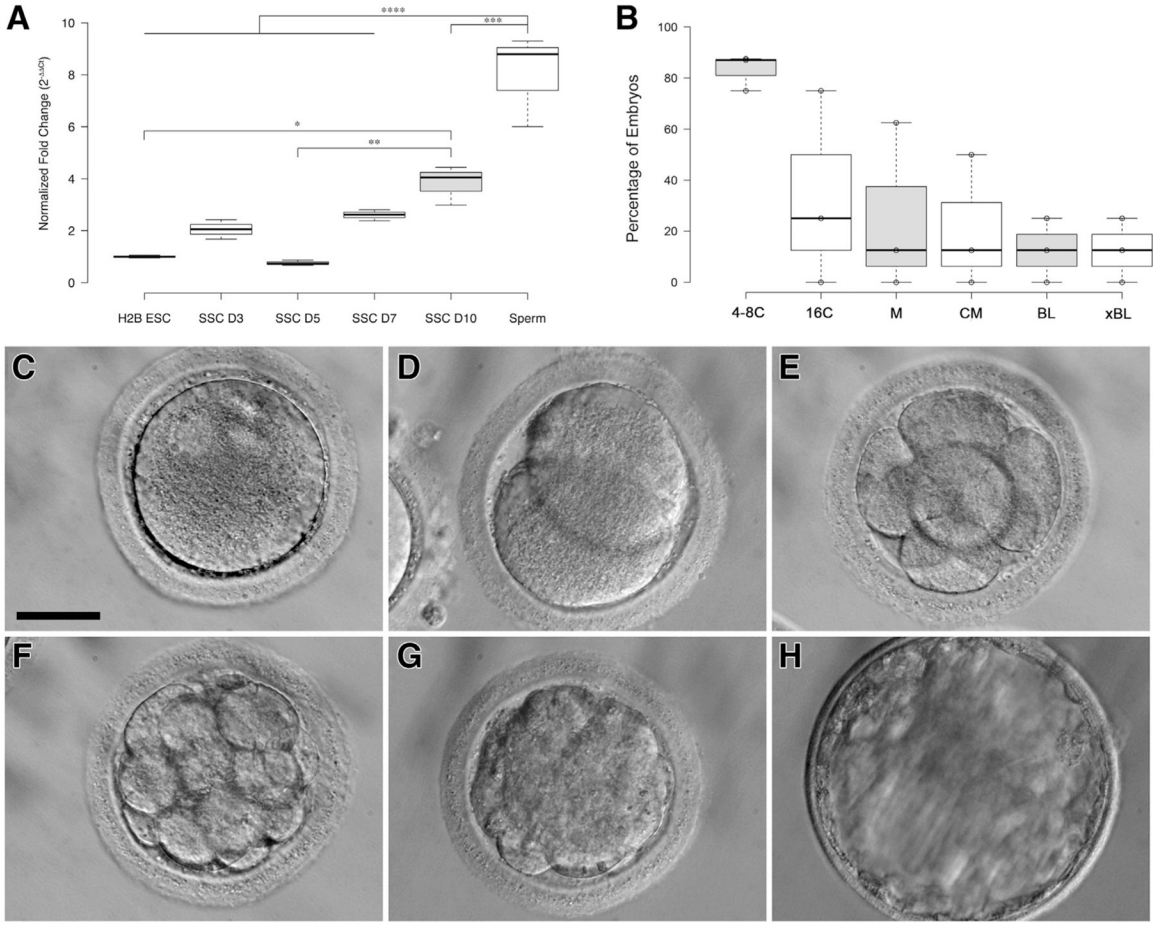

FIGURE 4.

Ten-eleven translocation 3 (TET3) protein injection and oocyte activation are required to achieve optimal fertilization and blastocyst development rates. (**A**) Spermatogonial stem cell-mediated germ cell differentiation does not elevate *TET3* gene expression to levels observed in rhesus sperm (P=.0004). However, round spermatid-like cells (rSLCs) show significantly higher *TET3* expression compared with histone 2B embryonic stem cells (P=.01). Normalized fold change ($2^{-\delta\delta CT}$) for *TET3* from three separate differentiations and three different semen collections from one rhesus macaque (n = 3) is shown. Significantly different, *P<.05, **P<.005, ***P<.0005, ****P<.0001. (**B**) Graphical representation of the percentage of embryos that reach each developmental/postfertilization stage including the 4–8-cell (4–8C), 16-cell (16C), morula (M), compacted morula (CM), early blastocyst (BL), and expanded blastocyst (xBL) stages when in vitro-derived rSLCs are coinjected with TET3 protein and activated by sperm cell factor (SCF) (n = 25 embryos assessed). (**C**–**H**) Representative images of a developing embryo after fertilization with rSLCs from nonhuman primate embryonic stem cell histone 2B-green fluorescent protein cells coinjected with TET3 and SCF. Images show the zygote stage (**C**), two-cell stage (**D**), eight-cell stage (**E**), morula (**F**), CM (**G**), and expanded blastocyst (**H**). Bar = 100 μm.